Kathford Journal of Engineering and Management,
ISSN: 2661-6106.

https://kathford.edu.np/Journal/

VOL. 4 ISSUE 1 DECEMBER 2024, PP. 92-101

Use of Polynomial Mode Shape Function in Free Vibration Analysis of Cantilever Pelton Turbine

Bikki Chhantyal[1], Manoj Adhikari[1, *], Bir Bahadur Chaudhary[2], Mahesh Chandra Luintel[2]

[1]*Department of Mechanical Engineering, Thapathali Campus, Institute of Engineering, Tribhuvan University, Thapathali, Kathmandu, Nepal*
[2]*Department of Mechanical Engineering, Pulchowk Campus, Institute of Engineering, Tribhuvan University, Pulchowk, Kathmandu, Nepal*

Corresponding author: *manoj.adhikari@tcioe.edu.np*

ABSTRACT— In this study, we investigate the use of polynomial mode shape functions in the free vibration analysis of a cantilever Pelton turbine and compare it with the conventional transcendental mode shape function. The mathematical model is developed using the assumed mode method and Lagrange's equation, incorporating rotational inertia and centrifugal effects. Variable mode shapes and critical frequencies are determined using both polynomial and transcendental functions, and are compared exclusively. The results show that polynomial mode shape functions closely approximate the first mode shape but the deviation increases in higher modes, with a critical frequency deviation of 2.23% in the first mode and 14.58% in the second mode and 20.53% in the third mode. These findings suggest that while the polynomial mode shape functions offer computational simplicity, their accuracy decreases in complex rotor-dynamic systems. We can use polynomial mode shape function is case of simple dynamics and problems in which higher modes are negligible. Being the Cantilever Pelton Turbine complex, presently designed mathematical model and its outcomes are fully vowed to explain its vibrational consequences for first mode. The authors believe that the findings obtained through this theoretical work are applicable not only to Cantilever Pelton turbines but also to other rotor-dynamic systems with similar boundary conditions, such as turbine blades, flexible shafts, and cantilevered rotor structures in hydro and wind energy applications.

KEYWORDS— Transcendental Mode Shape Function, Shaft-Disk System, Campbell Diagram, Rotor Dynamics

1. INTRODUCTION

Vibration analysis is important in rotor-dynamics to ensure its operational reliability and performance relating to structural integrity, resonance avoidance, fatigue life, noise reduction, and overall efficiency of rotating machinery. The American Petroleum Institute (API) standard specifies that critical speeds of turbine should be at least 20% above the maximum operating speed or 15% below the minimum operating speed (Yong-Jun, 2009). If critical speed falls within this range, the excessive vibration can be observed. Excessive vibration can lead to detrimental effects including premature wear and tear on components, reduced efficiency, potential catastrophic failure of the rotating machinery, instability at critical speeds, increased noise levels etc.

The vibration analysis starts with mathematical modeling, where governing equations of motion are derived generally using energy methods. For discrete system, these equations are in ordinary differential equations whereas, for continuous systems, these equations are in the form of partial differential equation (hereafter, PDE) or system of PDEs. Analytical solutions of these PDEs to obtain natural frequencies and mode shapes essential to understand critical speed is possible in simple and special cases. However, systems with complex geometries, material properties, or dynamic coupling frequently result in non-standard PDEs. In such cases, numerical methods, including the Rayleigh-Ritz

method (Storch, & Strang, 1988), Galerkin technique (Hutton, 1971), or finite element analysis can be used relying on predefined spatial shape functions that approximate the system's mode shapes while satisfying geometric boundary conditions.

The mode shape function should show deformation pattern specific to natural frequency. They should satisfy boundary conditions inclusive with orthogonality conditions. Hence, they are specific to boundary conditions like clamped-clamped, clamped-free or simply supported. For the simply supported beam, the sine function mode shape is accurate, which is relatively easier than clamped-free boundary condition in which the transcendental mode shape function is complex (SS Rao, 2011). Despite its complexity in calculation, research articles reported elsewhere (Egusquiza et. al., 2017; Chaudhary et. al., 2024) have used transcendental mode shapes for the clamped-free boundary condition. Using complex mode shape function has made calculations computationally intensive and verification with hand calculation unlikely. To solve this problem, researchers have developed polynomial mode shape function for different boundary conditions in case of rotating beam (Luintel, 2021; Chen and Griffith, 2022).

In this paper, we compare the result of both mode shape functions in case of cantilever Pelton turbine. It can be assumed cantilever shaft with disk attached at its end. The rotary and centrifugal effects of disk is put in equation of motion using Dirac delta function.

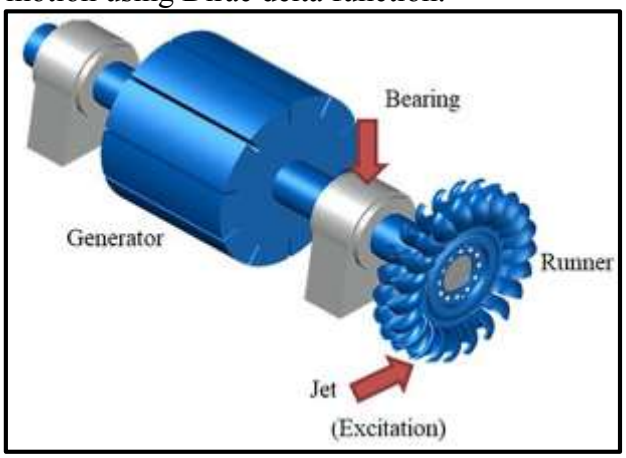

Figure 1. Pelton Turbine Assembly (Zhao *et. al.*, 2021)

2. MATHEMATICAL AND THEORETICAL DETAILS

For this paper, the axes x, y and z are chosen so that y is along the shaft's transverse axis on the vertical plane, z is along the shaft's transverse axis on the horizontal plane and x is along the shaft's longitudinal axis.

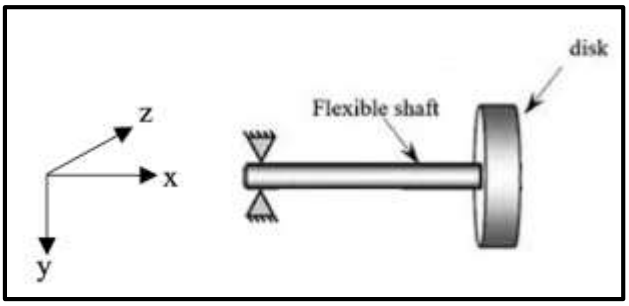

Figure 2. Cantilever Shaft-Disk

Similar to this, each point on the shaft's transverse displacements in both the horizontal and vertical directions are v(x,t) and w(x,t), respectively. The y-axis of water jet force applies on the horizontal shaft Pelton turbine. In this study, disk and bearing are assumed as rigid and shaft as flexible. Total kinetic and potential energy is calculated for shaft-disk system and with the help of assumed mode method and Lagrange's equation of motion, governing equation of motion is obtained which is second order coupled differential equation.

2.1 Kinematics of Shaft-Disk System

Velocity vector of any point on neutral axis of the flexible shaft is (Meirovitch, 2001)

$$v_s = (\dot{u} - \Omega v)\,\vec{j} + (\dot{v} + \Omega u)\,\vec{k} \qquad \ldots(1)$$

Angular velocity of disk is:

$$\omega_d = (\Omega + v'\dot{w}')\,\vec{i} + (-\Omega v' - \dot{w}')\,\vec{j} + (-\Omega w' + \dot{v}')\,\vec{k} \qquad \ldots(2)$$

2.2. Energy Method

2.2.1 Total Kinetic Energy of Shaft-Disk System

Kinetic energy of the shaft is sum of the translational and rotational kinetic energy which is given by following relation.

$$T_s = \frac{1}{2}\rho_s A \int_0^L [(\dot{v} - \Omega w)^2 + (\dot{w} + \Omega v)^2]\, dx + \frac{1}{2}\rho_s J_s \int_0^L [(\Omega + v'\dot{w}')^2]\, dx + \frac{1}{2}\rho_s I_s \int_0^L [(-\Omega v' - \dot{w}')^2 + (-\Omega w' + \dot{v}')^2]\, dx \quad \ldots(3)$$

Kinetic energy of the disk is sum of the translational and rotational kinetic energy which is given by following relation (Meirovitch, 2001).

$$T_d = \left[\frac{1}{2}[m_d\,[(\dot{v} - (\Omega w)^2 + (\dot{w} + \Omega v)^2] + \frac{1}{2}\rho_d h\, J_d(\Omega + v'\dot{w}')^2 + \frac{1}{2}\rho_d h\; I_d(-\Omega v' - \dot{w}')^2 + \frac{1}{2}\rho_d h\, I_d(-\Omega w' + \dot{v}')^2)\right]\Big|_{x=L} \quad \ldots(4)$$

Total kinetic energy of the shaft-disk system is sum of kinetic energy of the shaft and disk which is given by equation 5.

$$T = T_s + T_d \quad \ldots(5)$$

2.2.2 Total Potential Energy of Shaft-Disk System:

Since the shaft of the turbine is shaft is assumed as flexible, the strain energy of the shaft due to bending is given by following relation [8].

$$V_s = \frac{1}{2} EI_s \int_0^L [(v'')^2 + (w'')^2] dx \quad \ldots(6)$$

Since the disk is assumed as rigid, its potential energy of disk is zero.

Mathematically, $V_d = 0$,

Total potential energy of the shaft-disk system is sum of the potential energy of the shaft and disk which is given by

$$V = V_s + V_d \quad \ldots(6)$$

2.2.3 Assumed Mode Method

Using the assumed mode method, displacement variable is (Karki et. al., 2017)

$$v = \{\phi(x)\}^T \{V(t)\} = \{\phi\}^T \{V\}$$

$$w = \{\phi(x)\}^T \{W(t)\} = \{\phi\}^T \{W\} \quad \ldots(8)$$

Total kinetic and potential energies and external work done are discretized using Eq. 6, then applied in Lagrange's equation of motion.

2.2.4 Lagrange's Equation of Motion:

Simplified equation of motion can be derived using Lagrange's equation as:

$$\frac{d}{dt}\left(\frac{\partial T}{\partial \dot{q}}\right) - \frac{\partial T}{\partial q} + \frac{\partial V}{\partial q} = 0 \quad \ldots(9)$$

After simplification, we get following governing equation of motion:

$$M_i \ddot{V} + C_i \dot{W} + K_i V = 0$$
$$M_i \ddot{W} - C_i \dot{V} + K_i W = 0 \quad \ldots(10)$$

Where, equivalent parameters are as follows:

$$M_i = \rho_s A \int_0^L [\{\phi\}\{\phi\}^T] dx + \rho_s I_s \int_0^L [\{\phi'\}\{\phi'\}^T] dx + m_d \left[\{\phi\}_d \{\phi\}_d^T\right]_{x=L} + \rho_d h I_d \left[\{\phi'\}_d \{\phi'\}_d^T\right]_{x=L} \quad \ldots(11)$$

$$C_i = 2\rho_s A\Omega \int_0^L [\{\phi\}\{\phi\}^T] dx + 2\rho_s I_s \Omega \int_0^L [\{\phi'\}\{\phi'\}^T] dx + 2m_d \Omega [\{\phi_d\}\{\phi_d\}^T]_{x=L} + 2\rho_d h I_d \Omega \left[\{\phi'\}_d \{\phi'\}_d^T\right]_{x=L} + \rho_s J_s \Omega \int_0^L [\{\phi'\}\{\phi'\}^T] dx + \rho_d h J_d \Omega \left[\{\phi'\}_d \{\phi'\}_d^T\right]_{x=L} \quad \ldots(12)$$

$$K_i = -\rho_s A\Omega^2 \int_0^L [\{\phi\}\{\phi\}^T] dx - \rho_s I_s \Omega^2 \int_0^L [\{\phi'\}\{\phi'\}^T] dx - m_d \Omega^2 \left[\{\phi\}_d \{\phi\}_d^T\right]_{x=L} - \rho_d h I_d \Omega^2 \left[\{\phi'\}_d \{\phi'\}_d^T\right]_{x=L} + EI_s \int_0^L [\{\phi''\}\{\phi''\}^T] dx \quad \ldots(13)$$

2.2.5 Whirl frequencies from Mathematical Model

After putting values from Eqs. 11,12 and 13 into 10, we get two values of angular speed. Let ω_f be forward whirling frequency and ω_b be backward whirling frequency then,

$$\omega_f = \sqrt{\frac{1}{2}\left[\left\{\left(\frac{C_i}{M_i}\right)^2 + 2\frac{K_i}{M_i}\right\} + \sqrt{\left(\frac{C_i}{M_i}\right)^4 + 4\left(\frac{C_i}{M_i}\right)^2\frac{K_i}{M_i}}\right]}$$

$$\omega_b = \sqrt{\frac{1}{2}\left[\left\{\left(\frac{C_i}{M_i}\right)^2 + 2\frac{K_i}{M_i}\right\} - \sqrt{\left(\frac{C_i}{M_i}\right)^4 + 4\left(\frac{C_i}{M_i}\right)^2\frac{K_i}{M_i}}\right]}$$

2.3. Development of Mode Shape Function

Boundary conditions associated with the continuous shaft systems for different end conditions are given below:

At $\boldsymbol{x = 0}$, the displacement and slope are zero.

$$\mathbf{v(0,t) = 0;\ v'(0,t) = 0; w(0,t) = 0; w'0\ (0,t)\ = 0}$$

At $\boldsymbol{x = L}$, the moment and shear force are zero.

$$\mathbf{v''(L,t) = 0; v'''(L,t) = 0;\ w''(L,t) = 0; w'''(L,t)\ = 0}$$

2.3.1 Transcendental Mode Shape Function

Transcendental mode shape functions are accurate analytical solution which we want to approximate using polynomial function (SS Rao, 2011). Frequency equations for the continuous shaft systems for fixed-free conditions is given below:

$$\mathbf{\cos \beta_i l \cosh \beta_i l = -1}$$

Then mode shape function is

$$\mathbf{\phi_i(x) = C_i[\sin \beta_i x - \sinh \beta_i x - \left(\frac{\sin \beta_i L + \sinh \beta_i L}{\cos \beta_i L + \cosh \beta_i L}\right)(\cos \beta_i x - \cosh \beta_i x)]} \quad \ldots(14)$$

Where,

$$\mathbf{\beta_1 L = 1.875104,}$$
$$\mathbf{\beta_2 L = 4.694091,}$$
$$\mathbf{\beta_3 L = 7.854757}$$

2.3.2. Polynomial Mode Shape

Since the highest order of derivative in the governing equation is four, the assumed polynomial mode shape function should have the order equal to or greater than 4. Hence for the first three modes, the mode shape functions can be assumed as:

$$\phi_1 = x^4 + A_3x^3 + A_2x^2 + A_1x + A_0$$

$$\phi_2 = x^5 + B_4x^4 + B_3x^3 + B_2x^2 + B_1x + B_0$$

$$\phi_3 = x^6 + C_5x^5 + C_4x^4 + C_3x^3 + C_2x^2 + C_1x + C_0$$

2.3.2.1 First Mode Shape

$$\phi_1 = x^4 + A_3x^3 + A_2x^2 + A_1x + A_0$$

All constants can be derived from boundary conditions alone.

$$\phi_i(0) = 0;\ \phi_i'(0) = 0;\ \phi_i''(L) = 0;\ \phi_i'''(L) = 0$$

From first condition:

$$\phi_1(0) = 0$$
$$(x^4 + A_3x^3 + A_2x^2 + A_1x + A_0)|_{x=0} = 0$$
$$x^4 + A_3(0)^3 + A_2(0)^2 + A_1(0) + A_0 = 0$$
$$\Rightarrow A_0 = 0$$

From second condition:

$$(x^4 + A_3x^3 + A_2x^2 + A_1x + A_0)'|_{x=0} = 0$$
$$4x^3 + 3A_3(x)^2 + 2A_2x + A_1 = 0$$
$$\Rightarrow A_1 = 0$$

From third condition:

$$\phi_1''(L) = 0$$
$$(x^4 + A_3x^3 + A_2x^2 + A_1x + A_0)''|_{x=L} = 0$$
$$(12x^2 + 6A_3x + 2A_2)''|_{x=L} = 0$$
$$12L^2 + 6A_3L + 2A_2 = 0$$

From fourth condition:
$\phi_1'''(L) = 0$
$(x^4 + A_3x^3 + A_2x^2 + A_1x + A_0)'''|_{x=L} = 0$
$(24x + 6A_3)|_{x=L} = 0$
$24\,L + 6A_3 = 0$
$A_3 = -4L$

Putting value of $A_3 = -4L$ in third condition;
$A_2 = 6L^2$

$$\phi_1 = x^4 - 4Lx^3 + 6L^2x^2 \qquad \ldots(15)$$

2.3.2.2 Second Mode Shape

$$\phi_2 = x^5 + B_4x^4 + B_3x^3 + B_2x^2 + B_1x + B_0$$

Here are five unknowns namely B_0, B_1, B_2, B_3 and B_4. Four equations will be obtained from the boundary conditions and one equation will be obtained from the orthogonality condition of first and second mode shape functions.

From first condition:
$\phi_1(0) = 0$
$(x^5 + B_4x^4 + B_3x^3 + B_2x^2 + B_1x + B_0)|_{x=0} = 0$

$$B_0 = 0 \qquad \ldots(16)$$

From second condition:
$(x^5 + B_4x^4 + B_3x^3 + B_2x^2 + B_1x + B_0)'|_{x=0} = 0$
$5x^4 + 4B_4(x)^3 + 3B_3x^2 + 2B_2x + B_1 = 0$

$$B_1 = 0 \qquad \ldots(17)$$

From third condition:
$\phi_1''(L) = 0$
$(x^5 + B_4x^4 + B_3x^3 + B_2x^2 + B_1x + B_0)''|_{x=L} = 0$
$(20x^3 + 12\,B_4x^2 + 6B_3x + 2B_2)''|_{x=L} = 0$

$$20L^3 + 12B_4L^2 + 6B_3L + 2B_2 = 0 \qquad \ldots(18)$$

From fourth condition:
$\phi_1'''(L) = 0$
$(x^5 + B_4x^4 + B_3x^3 + B_2x^2 + B_1x + B_0)'''|_{x=L} = 0$
$(60x^2 + 24\,B_4x + 6B_3)|_{x=L} = 0$
$60L^2 + 24B_4L + 6B_3 = 0$

$$60L^2 + 24B_4L + 6B_3 = 0 \qquad \ldots(19)$$

From orthogonality condition

$$\int_0^L \phi_1\phi_2\,dx = 0$$

$$\int_0^L (x^4 - 4Lx^3 + 6L^2x^2)(x^5 + B_4x^4 + B_3x^3 + B_2x^2)\,dx$$

$$\frac{73}{180}L^{10} + \frac{59}{126}L^9B_4 + \frac{31}{56}B_3L^8 + \frac{71}{105}L^7B_2 = 0 \qquad \ldots(20)$$

The values after solving Eqs. 16,17,18,19 and 20 is:

$$B_4 = -\frac{661}{182}L, B_3 = \frac{412}{91}L^2, B_2 = -\frac{163}{91}L^3$$

Hence, the mode shape function is:

$$\phi_2 = x^5 - \frac{661}{182}Lx^4 + \frac{412}{91}L^2x^3 - \frac{163}{91}L^3x^2 \qquad \ldots(21)$$

2.3.2.3 Third Mode Shape

$$\phi_3 = x^6 + C_5x^5 + C_4x^4 + C_3x^3 + C_2x^2 + C_1x + C_0$$

Four equations obtained from boundary conditions and two conditions obtained from orthogonality condition.

$$\int_0^L \phi_1\phi_3\,dx = 0$$

And,

$$\int_0^L \phi_2\phi_3\,dx = 0$$

The third mode shape is calculated using Maple as:

$$\phi_3 = x^6 - \frac{9953}{2608}Lx^5 + \frac{305815}{57376}L^2x^4 - \frac{5560}{1793}L^3x^3 + \frac{115}{176}L^4x^2 \quad \ldots(22)$$

3. RESULTS AND DISCUSSIONS

To have comparison of polynomial shape functions and the resulting critical frequencies with those for the classical transcendental shape functions for the shafts with different end conditions, different material and geometric properties of the shaft are taken as: shown in Table 1.

Table 1. Parameters for Pelton Turbine Model

Parameters	Value
Pitch diameter of disk (d_d)	180 mm
Rated angular speed (Ω)	157 rad/s
Diameter of shaft (d_s)	40 mm
Length of shaft (L)	135 mm
Cross section area of shaft (A)	0.0008042 m^2
Density of shaft material (ρ_s)	7860 kg/m^3
Density of disc material (ρ_d)	8300 kg/m^3
Young's Modulus of Elasticity of shaft (E)	202 GPa
Mass of rotating runner (m_d)	3.72 kg
Thickness of runner (h)	0.018 m
Area polar moment of inertia of shaft about z-z axis (J_s)	2.5133×10^{-7} m^4
Area moment of inertia of shaft about x-x or y-y axis (I_s)	1.2566×10^{-7} m^4
Area polar moment of inertia of disk about z-z axis (J_d)	0.0001028 m^4
Area moment of inertia of disk about x-x or y-y axis (I_d)	$5.14043\times10^{-5}m^4$

3.1. Mode Shapes

3.1.1 First Mode

Putting $\boldsymbol{x = \frac{x}{L}}$ then,

For transcendental mode shape function

$$\boldsymbol{\phi_1(x) = C_1[\sin 1.875104\,x - \sinh 1.875104\,x - \left(\frac{\sin 1.875104 + \sinh 1.875104}{\cos 1.875104 + \cosh 1.875104}\right)(\cos 1.875104\,x - \cosh 1.875104\,x)]}$$

In the range of 0 to 1, its maximum absolute value is 2.7244186.

So, normalized shape function is:

$$\boldsymbol{\phi_1(x) = \frac{1}{2.7244186}[\sin 1.875104\,x - \sinh 1.875104\,x - \left(\frac{\sin 1.875104 + \sinh 1.875104}{\cos 1.875104 + \cosh 1.875104}\right)(\cos 1.875104\,x - \cosh 1.875104\,x)]} \quad \ldots(23)$$

For polynomial mode shape function

$$\boldsymbol{\phi_1(x) = x^4 - 4x^3 + 6x^2}$$

In the range of 0 to 1, its maximum value is 3.

So, normalized shape function is:

$$\boldsymbol{\phi_1(x) = \frac{1}{3}[x^4 - 4x^3 + 6x^2]} \quad \ldots(24)$$

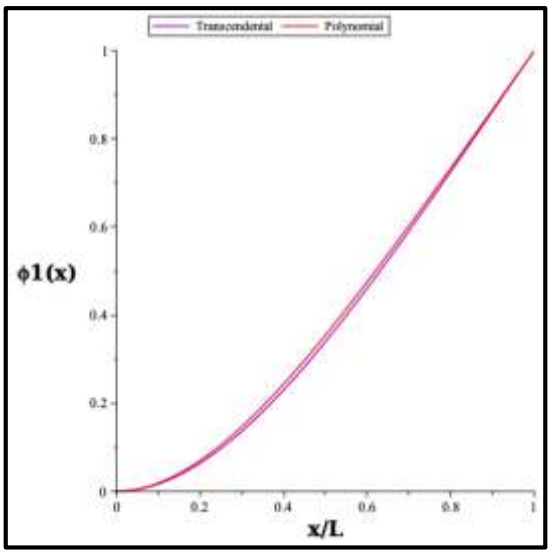

Figure 3. First Mode Shapes (Transcendental and Polynomial (Eqs. 23 and 24))

3.1.2 Second Mode

Putting $\boldsymbol{x = \frac{x}{L}}$ then,

For transcendental mode shape function

$$\boldsymbol{\phi_2(x) = C_2[\sin 4.694091\,x - \sinh 4.694091\,x - \left(\frac{\sin 4.694091 + \sinh 4.694091}{\cos 4.694091 + \cosh 4.694091}\right)(\cos 4.694091\,x - \cosh 4.694091\,x)]}$$

In the range of 0 to 1, its maximum absolute value is -1.4144.

So, normalized shape function is:

$$\boldsymbol{\phi_2(x)} = \frac{1}{1.4144}[\sin 4.694091\,x - \sinh 4.694091\,x - \left(\frac{\sin 4.694091+\sinh 4.694091}{\cos 4.694091+\cosh 4.694091}\right)(\cos 4.694091\,x - \cosh 4.694091\,x)] \quad \ldots(25)$$

For polynomial mode shape function $\boldsymbol{\phi_2(x) = x^5 - \frac{661}{182}x^4 + \frac{412}{91}x^3 - \frac{163}{91}x^2}$
In the range of 0 to 1, its maximum value is 0.08074.
So, normalized shape function is:

$$\boldsymbol{\phi_2(x)} = \frac{1}{-0.08074}\left[x^5 - \frac{661}{182}x^4 + \frac{412}{91}x^3 - \frac{163}{91}x^2\right] \quad \ldots(26)$$

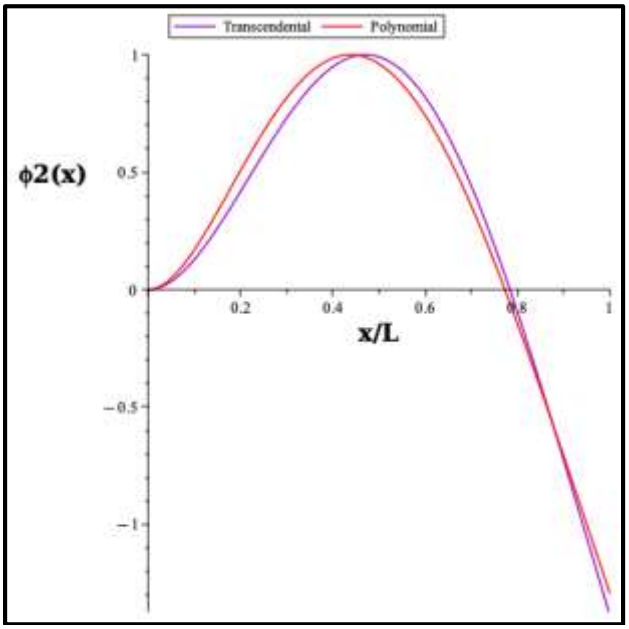

Figure 4. Second Mode Shapes (Transcendental and Polynomial (Eqs. 25 and 26))

3.1.3 Third Mode

Putting $\boldsymbol{x = \frac{x}{L}}$ then,
For transcendental mode shape function $\boldsymbol{\phi_2(x) = C_2[\sin 7.854757\,x - \sinh 7.854757\,x - \left(\frac{\sin 7.854757+\sinh 7.854757}{\cos 7.854757+\cosh 7.854757}\right)(\cos 7.854757\,x - \cosh 7.854757\,x)]}$
In the range of 0 to 1, its maximum absolute value is 2.0015513.
So, normalized shape function is:

$$\boldsymbol{\phi_2(x)} = \frac{1}{2.0015513}[\sin 7.854757\,x - \sinh 7.854757\,x - \left(\frac{\sin 7.854757+\sinh 7.854757}{\cos 7.854757+\cosh 7.854757}\right)(\cos 7.854757\,x - \cosh 7.854757\,x)] \quad \ldots(27)$$

For polynomial mode shape function
$\phi_3 = x^6 - \frac{9953}{2608}Lx^5 + \frac{305815}{57376}L^2x^4 - \frac{5660}{1793}L^3x^3 + \frac{115}{176}L^4x^2$

In the range of 0 to 1, its maximum absolute value is 0.010370.

$$\phi_3 = \frac{1}{0.010370}(x^6 - \frac{9953}{2608}Lx^5 + \frac{305815}{57376}L^2x^4 - \frac{5660}{1793}L^3x^3 + \frac{115}{176}L^4x^2) \quad \ldots(28)$$

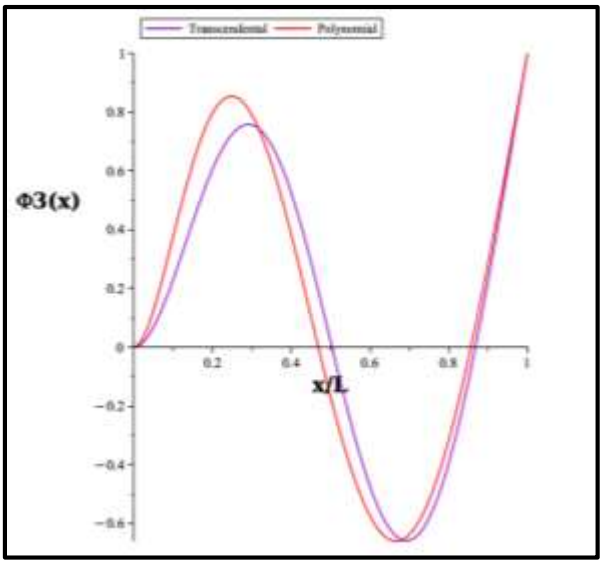

Figure 5. Third mode Shapes (Transcendental and Polynomial (Eqs. 27 and 28))

3.2 Campbell Diagram

Campbell diagram is used to observe the variation of natural frequencies with speed of the rotor. In this case, it is particularly important to obtain critical frequency.

3.2.1 First Mode

The critical frequency for first mode is calculated as:

Transcendental Mode Shape = 1225.42 rad/s
Polynomial Mode Shape = 1254.91 rad/s

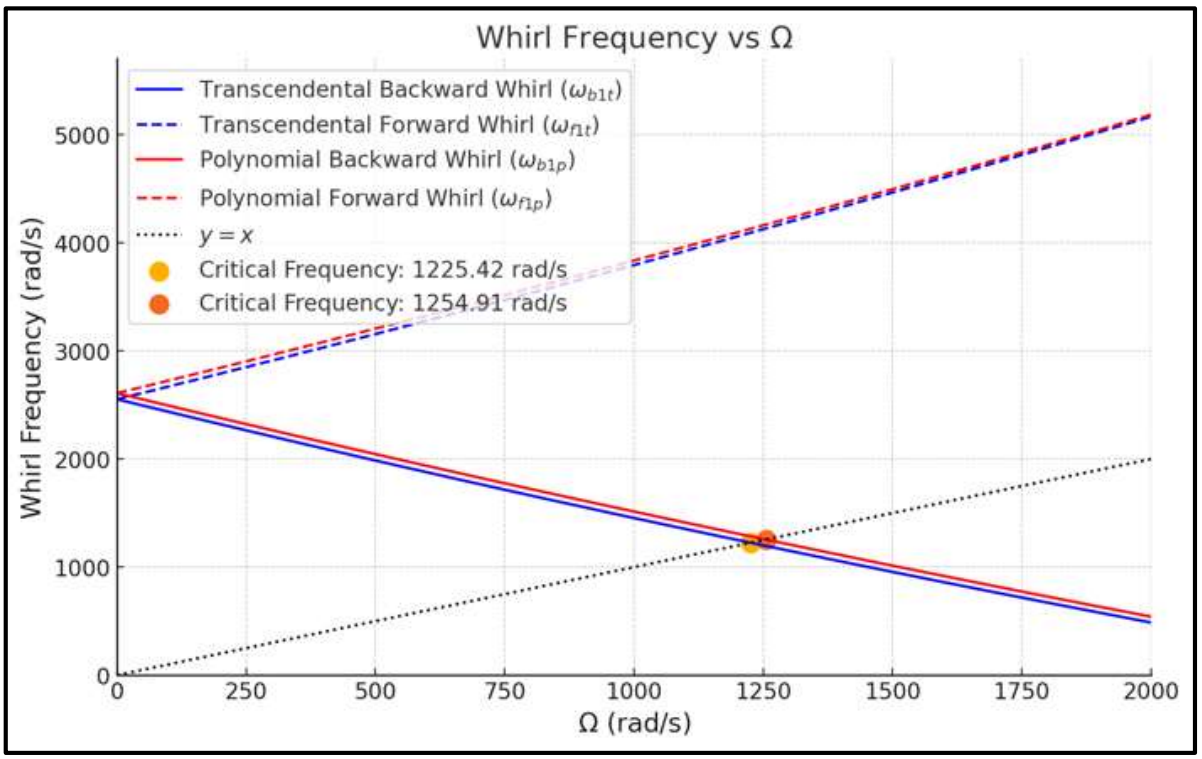

Figure 6. Campbell Diagram for First Mode Shape

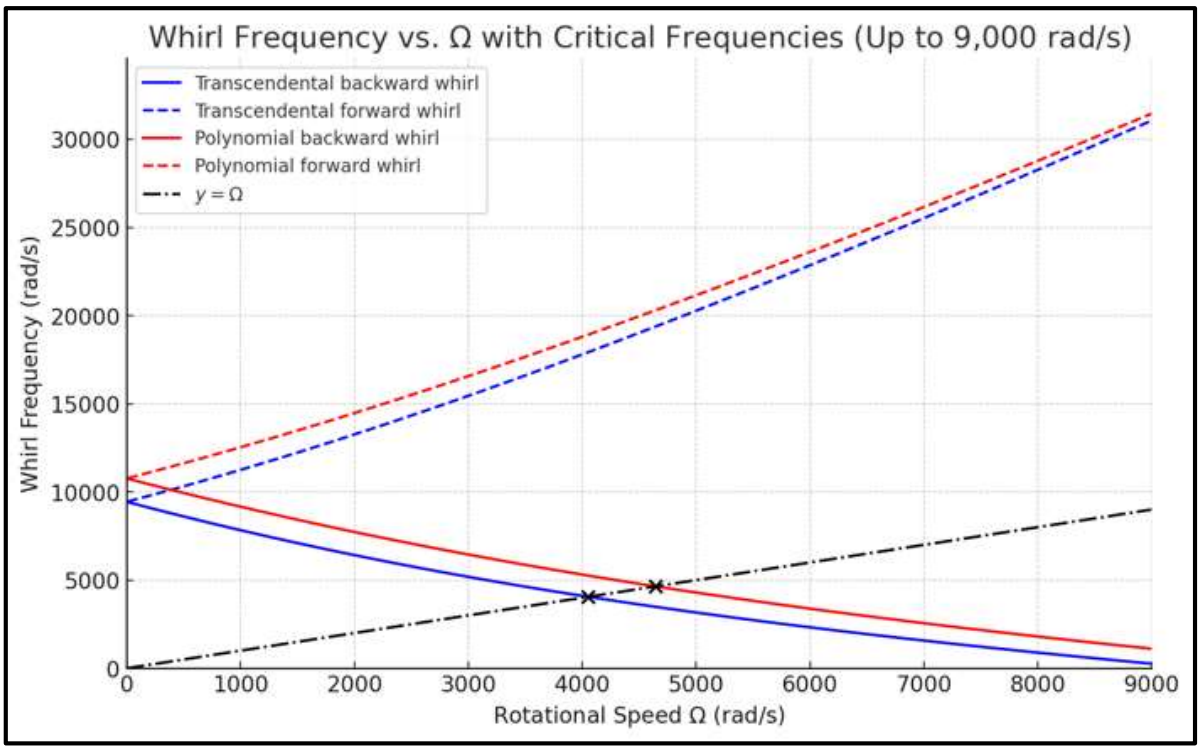

Figure 7. Campbell Diagram for Second Mode Shape

3.2.2 Second Mode

The critical frequency for second modes is:

Polynomial Mode Shape = 4645.16 rad/s
Transcendental Mode Shape = 4054.51 rad/s

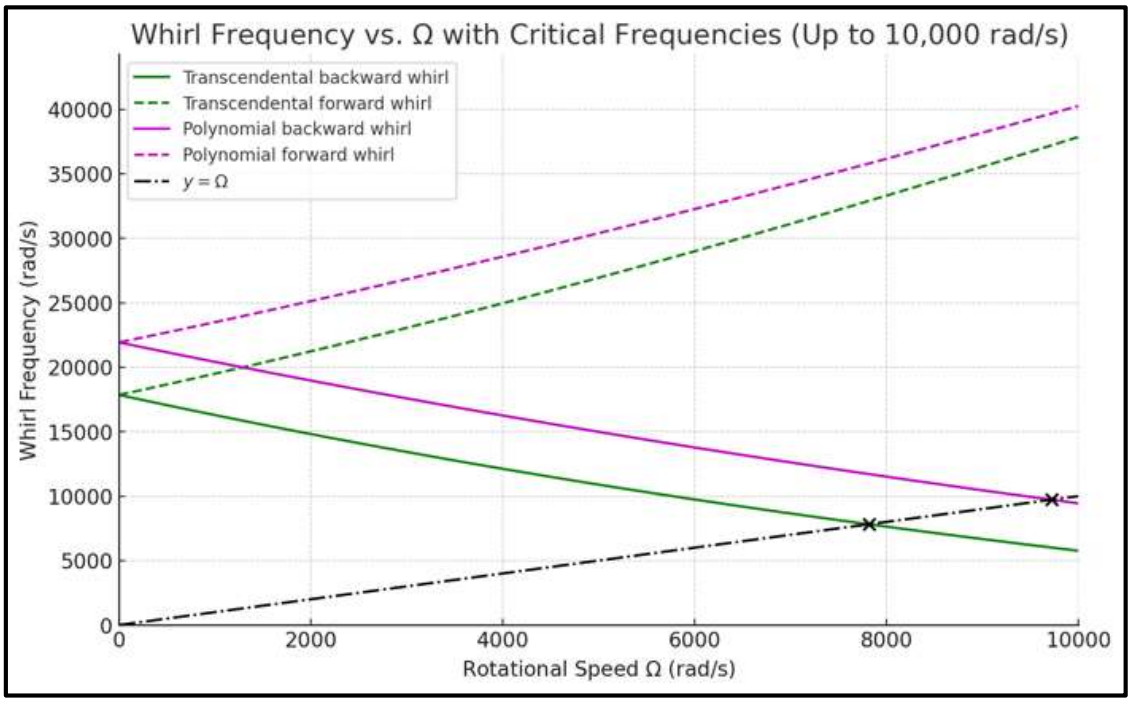

Figure 8. Campbell Diagram for Third Mode Shape

3.2.3 Third Mode

The critical frequency for third modes is:
Polynomial Mode Shape = 9415 rad/s
Transcendental Mode Shape = 7811 rad/s

3.3 Discussions

The mode shape function using transcendental and polynomial matches closely matches in the case of the first mode shape (Figure 3). However, the deviation increases in the second mode (Figure 4) and by the third mode (Figure 5), the deviation further increases. Campbell diagram is drawn to find critical frequency, which should be avoided. Figures 6,7,8 shows the backward and forward whirling frequencies for polynomial and transcendental mode shapes. The critical frequency differs by 2.23% for the first mode shape, but this difference increases to 14.58% for the second mode and further to 20.53% for the third mode. The inability of polynomial mode shapes to approximate transcendental mode shapes for higher mode is shown by the difference of critical frequencies for higher modes in Campbell diagram. Since the transcendental mode shapes are direct analytical solution for free vibration of cantilever rotor disk, due to approximation of this function by polynomial and hence closeness in critical frequency shows the correctness of method. Both the transcendental mode shape and polynomial mode shape perfectly satisfy the boundary condition i.e., displacement and slope zero in fixed end and shear force and moment zero in free end.

Gyroscopic and inertial forces are included in the equations of motion using Dirac delta function and hence, the boundary conditions are simplified and the usage is extended.

For lower mode, polynomial mode shape functions are good. However, for more higher modes, it is recommended to use transcendental mode shapes. Since the designed Pelton turbine operates outside the critical frequency range, it can operate without any significant vibrational problems. Other than Pelton turbines, this formulation is valid for the vibration analysis of machines, cutting tools and turbines with a fixed-free support. For the other boundary conditions, like simply supported or fixed-fixed, the polynomial shape functions have to be derived.

4. CONCLUSION

This study investigated the application of polynomial mode shape functions in the free vibration analysis of a cantilever Pelton turbine and compared the results with the established transcendental mode shape functions. The

findings indicated that while polynomial mode shape functions can approximate the first mode shape with reasonable accuracy, discrepancies arise in higher modes. The critical frequency derived from polynomial mode shapes differed by 2.23% for the first mode but increased to 14.58% for the second mode and 20.53% for the third mode. The results from the Campbell diagram further explained these differences suggesting that polynomial mode shapes are useful for simple cases but may not be reliable for complex rotating systems like the Pelton turbine. Given the increasing deviation in higher modes, transcendental mode shape functions are recommended for more accurate vibration analysis in such cases. In both the cases, the critical frequency is well above operating speed i.e., 157 rad/s. Hence, the Pelton turbine is safe to operate in this operating range.

NOMENCLATURE

E	Modulus of elasticity
m_d	Mass of disk
L	Length of shaft
Ω	Spin speed of shaft
ρ_s	Density of shaft
ρ_d	Density of disk
A	Cross section area of shaft
$v(t)$	Transverse(in-plane) displacement
I	Moment of inertia of shaft about *Y/Z*-axis
$w(t)$	Transverse(out-of-plane) displacement
J	Polar Moment of Inertia of shaft about X-axis
$\phi(x)$	Mode Shape Function
J_d	Polar Moment of Inertia of disk about X-axis
I_d	Moment of inertia of disk about Y/Z-axis

REFERENCES

1. Chaudhary, B. B., Chhantyal, B., & Luintel, M. C. (2024). Transient response analysis of simply supported Pelton turbine during starting and shutdown. *Journal of Innovations in Engineering Education*, 7(1), 124–130.

2. Chen, Y., & Griffith, D. T. (2022). Mode shape recognition of complicated spatial beam-type structures via polynomial shape function correlation. *Experimental Techniques*, 46(6), 905–917.

3. Egusquiza, M., Egusquiza, E., Valentin, D., Valero, C., & Presas, A. (2017). Failure investigation of a Pelton turbine runner. *Engineering Failure Analysis*, 81, 234–244.

4. Hutton, S. (1971). Finite element method - a Galerkin approach. *Journal of Engineering Mechanics-asce*, 97, 1503–1520.

5. Karki S, Luintel M, Poudel L. (2017) dynamic response of Pelton turbine unit for forced vibration[C]/ IOE Graduate Conference: volume 5, 509–517.

6. Luintel, M. C. (2021). Development of Polynomial Mode Shape Functions for Continuous Shafts with Different End Conditions. *Journal of the Institute of Engineering*, 16(1), 151–161.

7. Meirovitch L. Fundamentals of vibration. McGraw-Hill, 2001.

8. S. S. Rao, Mechanical Vibrations, U K: Pearson Education Limited, 2011.

9. Storch, J., & Strang, G. (1988). Paradox lost: Natural boundary conditions in the Ritz–Galerkin method. *International Journal for Numerical Methods in Engineering*, 26, 2255–2266.

10. Yong-Jun, C. (2009). Introduction of API Vibration Acceptance Standard for Turbine Machines. *Process Equipment & Piping*.

11. Zhao, W., Egusquiza, M., Estevez, A., Valentín, D., Bossio, M., & Presas, A. (2021). Improved damage detection in Pelton turbines using optimized condition indicators and data-driven techniques. *Structural Health Monitoring,* 20(6), 3239–3251.